Comparison of Integrating GF-7 and ICESat-2 Laser Altimetry Data with High-resolution Stereo Images for Stereo Mapping

Jiyi Chen [1], Guoyuan Li [1], Jinquan Guo [2], Jun Peng [1,3]

[1] Land Satellite Remote Sensing Application Center, Ministry of Natural Resources, Beijing, China, 100048
[2] Wuhan University, Wuhan, Hubei, China, 430072
[3] Shandong University of Science and Technology, Qingdao, Shandong, China, 266590

Keywords: GF-7 Satellite, ICESat-2, Stereo Mapping, Laser Altimetry, Combined Bundle Adjustment, Laser Elevation Control Point.

Abstract

Currently, two types of satellite laser altimetry systems are in operation: the full waveform linear system and the single-photon-counting system, which exhibit significant differences in both data format and processing methodologies. It remains uncertain which satellite laser altimetry technology offers greater advantages in assisting stereo mapping of high-resolution optical imagery. To evaluate the effectiveness of those two satellite laser altimetry technologies in supporting optical imagery stereo mapping, this study extracted laser elevation control points from both GF-7 satellite and ICESat-2 laser altimetry data, and designed a specialized bundle adjustment workflow for GF-7 satellite stereo images incorporating laser elevation control points. Comparative experiments were conducted across both flat and mountainous regions. Results demonstrate that laser elevation control points derived from both GF-7 satellite and ICESat-2 effectively improved the elevation accuracy of stereo mapping of GF-7 satellite images. However, the ICESat-2 laser altimetry data has advantages in quantity and distribution, and the combined bundle adjustment accuracy of the two survey areas is slightly better than that of the GF-7 satellite laser altimetry data.

1. Introduction

Satellite laser altimetry can obtain high-precision surface elevation information, which can serve as elevation control points to enhance the geometric accuracy of optical stereo images. It is an effective way to carry out high-precision mapping using satellite images in areas lacking ground control data. In recent years, satellite laser altimetry technology for Earth Observation has been developping rapidly. As a successor to ICESat-1(Schutz et al., 2005), NASA launched ICESat-2 in 2018, equipped with ATLAS(Advanced Topographic Laser Altimeter System), a next-generation satellite laser altimetry system utilizing single-photon laser altimetry technology (Neumann et al., 2019). In the same year, NASA deployed GEDI (Global Ecosystem Dynamics Investigation) on the International Space Station, implementing full-waveform laser altimetry technology comparable to that of ICESat-1 (Dubayah et al., 2020). In 2015, China conducted its first Earth observation laser altimetry experiment on ZY3-02 satellite, pioneering the exploration of integrative laser altimetry and stereo image mapping techniques (Li et al., 2018). After that, China launched GF-7 (Tang et al., 2020), ZY3-03 (Li et al., 2022) satellites in 2019 and 2020, both equipped with laser altimetry systems. All these provide an unprecedented opportunity for satellite laser altimetry data to assist stereo mapping of optical remote sensing images.

With the laser altimeter load, the elevation accuracy for the stereo mapping of the ZY3 satelites three-linear-array images was increased from about 15 m to 3 m (Li et al., 2018; Zhang et al., 2019). The GF-7 satellite is equipped with a two-beam laser altimetry system. Combined the laser altimetry data with two-linear-array images achieving sub-meter resolution, the stereo mapping of GF-7 satellite can meet the accuracy of China's 1:10000 scale mapping without ground control point (Chen et al., 2022; Tang et al., 2023).

ICESat-2 represents a significant technological advancement in satellite laser altimetry, employing innovative single-photon-counting technology that fundamentally differentiates its data acquisition methodology from ICESat-1 and the GF-7 satellite. For the ICESat-1 and GF-7 satellite, each laser emission generates an individual laser footprint and captures a comprehensive full-waveform signal. Surface characterization is achieved through sophisticated waveform analysis. In contrast, ICESat-2's single-photon-counting technology generates high-density photon clouds along the satellite's ground track, with terrain features and surface characteristics derived through sophisticated probabilistic distribution analysis of the photon spatial and temporal attributes. Despite not being specifically designed for mapping purposes, the high-accuracy laser altimetry data of ICESat-2 is naturally complementary to stereo mapping of optical remote sensing images. Studies have demonstrated the feasibility of extracting elevation control points from the ICESat-2 data product (Li B.B. et al., 2021; Wang et al., 2020). However, the potential of full-waveform laser altimetry data represented by GF-7 satellite and single-photon-counting laser altimetry data represented by ICESat-2 in assisting stereo mapping of optical remote sensing images has not been fully compared and evaluated. In this study, the laser elevation control points were extracted from GF-7 satellite and ICESat-2 laser altimetry data, respectively, and the combined bundle adjustment experiment was carried out by using GF-7 stereo images with the laser elevation control points in plain and mountainous areas, to evaluate the potential of two different systems of laser altimetry data in supporting stereo mapping.

2. Data and Study Area

This study selected data from two survey areas in the United States to conduct experiments: the State of Iowa (IA) and the Commonwealth of Pennsylvania (PA). The IA survey area is characterized by flat terrain, predominantly composed of agricultural farmland, whereas the PA survey ares features mountainous topography densely covered with vegetation. The experimental data includes ICESat-2 ATL08 data, GF-7 satellite laser altimetry data and stereo images. The spatial distribution of the experimental data is illustrated in Figure 1.

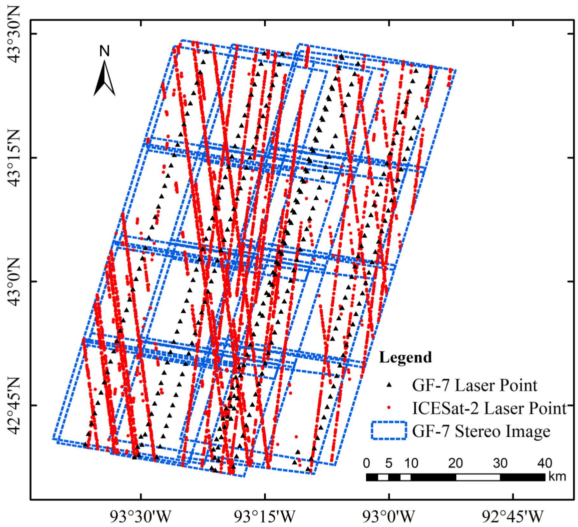

(a) IA survey area

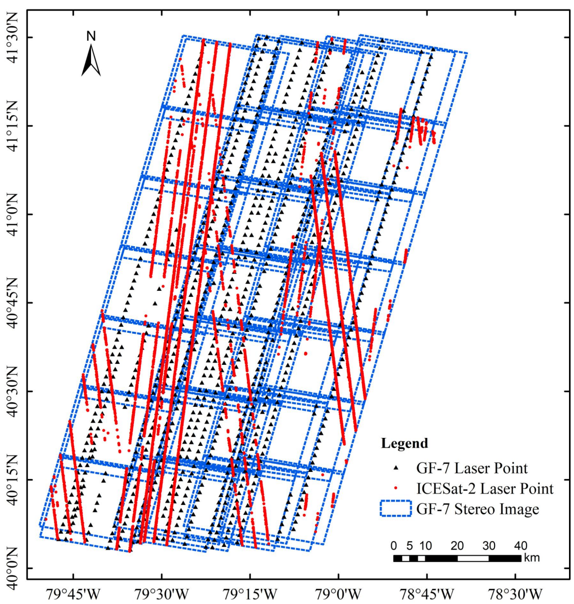

(b) PA survey area

Figure 1. Data distribution of the survey areas.

2.1 GF-7 Satellite Stereo Images

The stereo images from the GF-7 satellite includes both forward and backward views, with ground resolutions of 0.6 m and 0.8 m, respectively. In the IA survey area, three image acquisition tracks were selected, each comprising four stereo image pairs, acquired on March 14, 2021, January 13, 2022, and December 23, 2022. The geographic boundaries of the survey area extended from longitude -97.68° to -92.93° West and latitude 42.60° to 43.43° North, with elevation variations between 280m and 350m, typical of the Midwestern United States' flat agricultural terrain. Five image acquisition tracks in the PA survey area were selected, with each track containing seven stereo image pairs, acquired on September 21, 2020, January 22, 2021, March 22, 2021, May 20, 2021, and September 20, 2021. The geographic boundaries of the survey area extended from longitude -79.90° to -78.68°West and latitude 40.05° to 41.52° North, exhibiting substantial elevation variations between 200 m and 500 m, typical of the Appalachian Mountain region's complex terrain and dense vegetation..

2.2 GF-7 Satellite SLA03 Data

The GF-7 satellite SLA03 products, serving as the standard laser altimetry data products, were employed in this study. These products were generated through a comprehensive processing workflow utilizing precise orbital and attitude data, on-orbit calibration measurements, and supplementary external information. The processing workflow encompassed critical procedures including full-waveform decomposition, geometric positioning, footprint image process and environmental corrections such as atmospheric delay and tidal effects(Li G.Y. et al., 2021). These standard products include full-waveforms, footprint images, geometric coordinates of laser footprints, and various feature parameters. Most of the SLA03 products were collected synchronously with the stereo images.

2.3 ICESat-2 Satellite ATL08 Data

Data acquired by ICESat-2 are produced into a series of data products, from ATL01 to ATL23. These products are widely applied in measuring height changes of ice sheets and glaciers, retrieving forest vegetation heights, and monitoring lake water levels, all of which provide a reliable data source for global climate change research.

As a fundamental data product of the ICESat-2 satellite mission, the ATL08 data products offer comprehensive insights into terrestrial topography and vegetation morphology, enabling detailed spatial analysis of land surface and canopy height parameters (Neuenschwander et al., 2019). More information can be found in the official documentation(Algorithm Theoretical Basis Document for ATL08, V06).

The ATL08 data acquisition for the Iowa (IA) survey area spanned the period from April 2020 to December 2020, while in the Pennsylvania (PA) survey area data were collected between November 2019 and May 2020.

2.4 Reference Data for Accuracy Evaluation

High accuracy ground control data is necessary for evaluation. In this study, ground checkpoints were manually collected from air-borne LiDAR data, which was provided by the USGS (https://apps.nationalmap.gov/lidar -explorer/#/). For the IA and PA survey areas, 27 and 30 evenly distributed high-precision checkpoints were manually selected, respectively, and their coordinates were transformed into the coordinate system of the GF-7 satellite and ICESate-2 data.

3. Methods

3.1 Extraction of GF-7 Laser Elevation Control Points

The laser altimetry system onboard the GF-7 satellite collects full-waveform data, which provides critical insights into the Earth's surface characteristics. The shape of full-waveforms is dynamically altered by key factors including surface topography, terrain roughness, and surface objects. In flat areas, the full-waveform of laser points typically manifests as a single-peaked Gaussian-shaped waveform. In contrast, laser points in areas with vegetation, surface objects, or rugged terrain often exhibit broadened or multiple peaks waveforms, as shown in Figure 2. First, laser points with waveform exhibiting a single peak and a full width at half maximum (FWHM) that was not significantly broadened were selected. This selection criterion helps to identify points that were likely to be located in areas with relatively simple topography, thereby enabling high elevation accuracy. Subsequently, based on the land cover types where the laser points were located, further filtering was performed, eliminating laser points from water bodies and artificial surfaces. In addition, laser points with low signal-to-noise ratios or saturated waveforms, which were already recognized in the SLA03 data products, were also excluded. Through these procedures, high-precision laser elevation control points were extracted from the SLA03 data products of the GF-7 satellite (Li G.Y. et al., 2021).

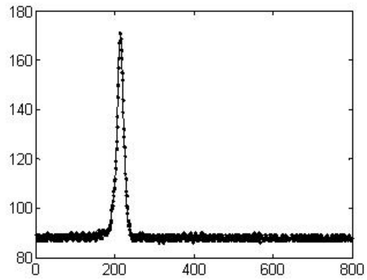

(a) Flat areas without vegetation or artificial objects

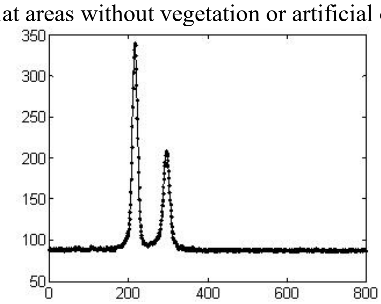

(b) Flat areas with artificial objects

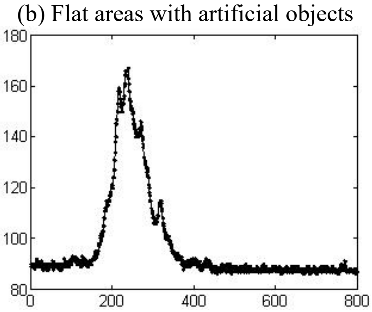

(c) Rugged terrain or vegetated areas

Figure 2. Typical waveforms of GF-7 satellite in different areas.

3.2 Extraction of ICESat-2 Laser Elevation Control Points

ICESat-2 laser elevation control points were extracted from ATL08 data products, which provide numerous key parameters regarding topography. The DEM (Digital Elevation Model) values provided in the ATL08 data products were employed to filter out points that are evidently in error. Similar to the extraction of GF-7 laser elevation control points, land cover information was also utilized as a reference to eliminate points classified as water bodies, forests, or unknown types. Then, photon feature parameters such as the number of photons within the footprint, the proportion of photons within the footprint, photon confidence, and the number of background noise photons were utilized to perform further filtering, retaining laser points that were minimally affected by atmospheric conditions and background environment, ensuring reliable elevation accuracy. In generally, the higher the proportion of ground photons in ICESat-2 laser altimetry data, the more accurate the calculated terrain elevation will be. Therefore, only segments with a proportion of ground photons greater than 50% were retained. The ATL08 products are divided into 100m segments, and each segment is further divided into 20m units known as geosegments. The best fit value is obtained by fitting the photon heights within each geosegment. To ensure the reliability of the elevation values, only geosegment where elevation values were all present in five segmentswere retained. Additionally, if the difference between the best fit values within the segment exceeded a threshold of 0.5 m, the data would be execluded. Combining the above strategies, the ICESat-2 satellite laser elevation control points were extracted.

3.3 Laser Elevation Control Points Supported Bundle Adjustment of Stereo Images

Bundle adjustment is an effective technique for enhancing the accuracy of stereo mapping by simultaneously optimizing multiple geometric parameters. The method involves three critical steps: first, identifying and matching corresponding points across stereo image pairs; second, formulating error equations that incorporate the rational function model (RFM) parameters, image and object coordinates of the corresponding points; and third, applying least squares optimization to simultaneously estimate both the refined RFM parameters and precise ground coordinates of the corresponding points.

The geometric relationship of coordinates on images and ground can be represented by the rational function model (Fraser and Yamakawa, 2004) as equation (1):

$$\begin{cases} x = \dfrac{Num_S\left(P,L,H\right)}{Den_S\left(P,L,H\right)} \\ y = \dfrac{Num_L\left(P,L,H\right)}{Den_L\left(P,L,H\right)} \end{cases} \tag{1}$$

where x, y = image coordinates (Normalized)
P, L, H = object coordinates (Normalized)
Num_S, Den_S, Num_L, Den_L = general third-order polynomials derived from parameters of the rational function model, known as Rational Polynomial Coefficients (RPC)

Geometric positioning errors can be compensated for by incorporating an affine transformation model in image space:

$$\begin{cases} \Delta x = a_0 + a_1 x + a_2 y \\ \Delta y = b_0 + b_1 x + b_2 y \end{cases} \tag{2}$$

where x, y = image coordinates
Δ x, Δ y = compensation values of image coordinates
a_0, a_1, a_2, b_0, b_1, b_2 = RPC compensation parameters

By combining equations (1) and (2) and performing linearization, the error equations for the corresponding points can be established as:

$$V_1 = A_1 t - B_1 x_1 - L_1 \tag{3}$$

where t = matrix consist of parameters of affine transformation model

https://doi.org/10.5194/isprs-annals-X-G-2025-165-2025 | © Author(s) 2025. CC BY 4.0 License.

x1 = matrix consist of object coordinates of the corresponding points
A_1, B_1 = coefficient matrix of unknown parameters
L_1 = constant term matrix of the corresponding points
V_1 = residual matrix the corresponding points

To incorporate laser elevation control points into the bundle adjustment process, the laser points should be matched onto the stereo images. For the GF-7 satellite laser elevation control points, a laser footprint image was available for each laser point and the position of the laser point on the footprint image was provided based on the internal geometry of the instruments (Huang et al., 2020; Li G.Y. et al., 2021). Therefore, it can be done by match the footprint image with the stereo images (Chen et al., 2022). For the ICESat-2 laser elevation control points without footprint images, the points were simply projected onto one of the stereo image with the lest view angle, and then matched onto the other stereo images. The matching flowchart is shown in Figure 3.

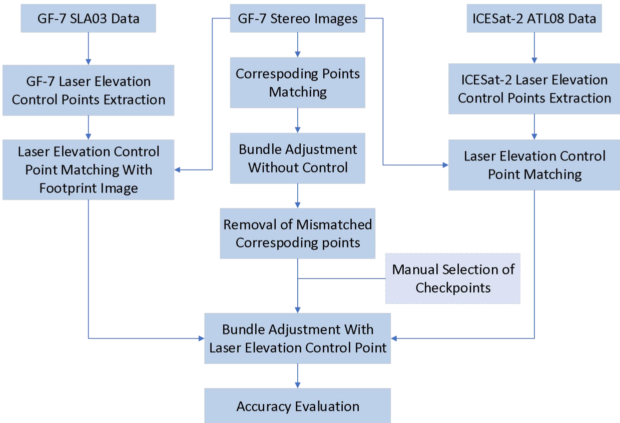

Figure 3. Flowchart of laser elevation control points supported bundle adjustment of stereo images.

The laser elevation control points can be viewed as corresponding points with know elevation, directly measured by the laser altimeter's high-precision ranging capabilities.

$$V_2 = A_2 t - B_2 x_2 - L_2 \tag{4}$$

where x2 = matrix consist of object coordinates of the laser elevation control points
A_2, B_2 = coefficient matrix of unknown parameters
L_2 = constant term matrix of the laser elevation control points
V_2 = residual matrix of the laser elevation control points

By combining the two types of error equations as equation (3) and (4), the RPC compensation parameters of the images and the object coordinates of the laser points (horizontal only) and corresponding points were solved using the least squares method.

4. Results

From the GF-7 satellite SLA03 products, 305 and 901 laser elevation control points were extracted in IA and PA survey areas, respectively. After the matching and blunder removal process, 107 and 145 GF-7 laser elevation control points were retained for the bundle adjustment. For the ICESat-2 ATL08 data, 5113 and 5229 laser elevation control points were obtained, and 400 and 350 points were used for the bundle adjustment in IA and PA survey areas, respectively.

Table 1 and Table 2 present comparative accuracy assessments of bundle adjustments for two-line array stereo image of GF-7 satellite across two distinct survey areas, demonstrating results obtained without laser elevation control points, with GF-7 satellite laser elevation control points, and with ICESat-2 laser elevation control points. The results reveals that while the horizontal accuracy of the bundle adjustments changes little before and after incorporating the laser elevation control points, the vertical accuracy demonstrates a significant improvement. The elevation accuracy of IA survey area was increased from 3.720 m to 0.787 m, and that of PA survey area was increased from 1.984 m to 1.005 m. Moreover, the maximum elevation errors were significantly reduced, especially in IA survey area, which dropped from 10.904 m to within 3.5 m. Both experiments demonstrated that the combined bundle adjustment utilizing laser elevation control points from ICESat-2 and GF-7 laser altimetry data, integrated with GF-7 satellite stereo images can meet the accuracy requirements of China's 1:10000 scale stereo mapping.

Comparative analysis of the combined bundle adjustment results from GF-7 and ICESat-2 laser elevation control points reveals nuanced differences in geometric accuracy: while the horizontal positioning precision was marginally superior with GF-7 laser control points, the vertical height accuracy demonstrated slightly better improvement using ICESat-2 control points across both survey areas. This may because that the laser footprint images would help to improve the horizontal accuracy, whereas the dense distribution of ICESat-2 data contribute to enhance the elevation accuracy.

Satellite	Laser Elevation Control Points	Ground Check Points	X RMSE/m	Y RMSE/m	Z RMSE/m	Z Max Error/m
/	0	27	3.589	3.007	3.720	10.904
GF-7	107	27	3.713	2.735	1.210	3.402
ICESat-2	400	27	5.028	2.466	0.787	1.398

Table 1. Bundle adjustment results of IA survey area

Satellite	Laser Elevation Control Points	Ground Check Points	X RMSE/m	Y RMSE/m	Z RMSE/m	Z Max Error/m
/	0	30	1.670	5.277	1.984	3.403
GF-7	145	30	1.582	3.314	1.372	3.308
ICESat-2	359	30	1.717	3.168	1.005	2.322

Table 2. Bundle adjustment results of PA survey area

Figure 4 shows the geometric errors of checkpoints after bundle adjustment of the GF-7 satellite stereo images in the absence of laser elevation control point. Figure 5 illustrates the geometric errors after integrating the laser elevation control points derived from the GF-7 SAL03 data with the stereo images. Figure 6 presents the geometric errors resulting from combining the laser elevation control points extracted from the ICESat-2 ATL08 data with the GF-7 satellite stereo images. Figure 4 reveals a systematic inclination of the terrain elevation from northwest to southeast across the two survey areas after bundle adjustment without laser elevation control points.

By comparing Figure 4 and Figure 5, it can be seen that incorporating laser elevation control points from the GF-7 satellite effectively mitigated the elevation inclination trend. However, due to the uneven spatial distribution of the laser elevation control points, a residual degree of inclination persisted even after combined bundle adjustments. In the IA survey area, the laser elevation control points are insufficient in the southeast region, resulting in a persistent southeast-northwest elevation tilt during the adjustment process. Similarly, in the PA survey area, the laser altimeter control points on the east and west sides were insufficient, the elevation accuracy was superior in the middle and poor at the periphery.

Figure 6 demonstrates that the incorporation of the ICESat-2 laser elevation control points effectively mitigated the previously observed systematic errors, substantially reducing their magnitude and impact. In comparison, ICESat-2 laser altimetry data demonstrates superior effectiveness in supporting the combined bundle adjustment, yielding a more uniform elevation error distribution. This improvement can be primarily attributed to the higher point density and more even distribution of the ICESat-2 laser elevation control points.

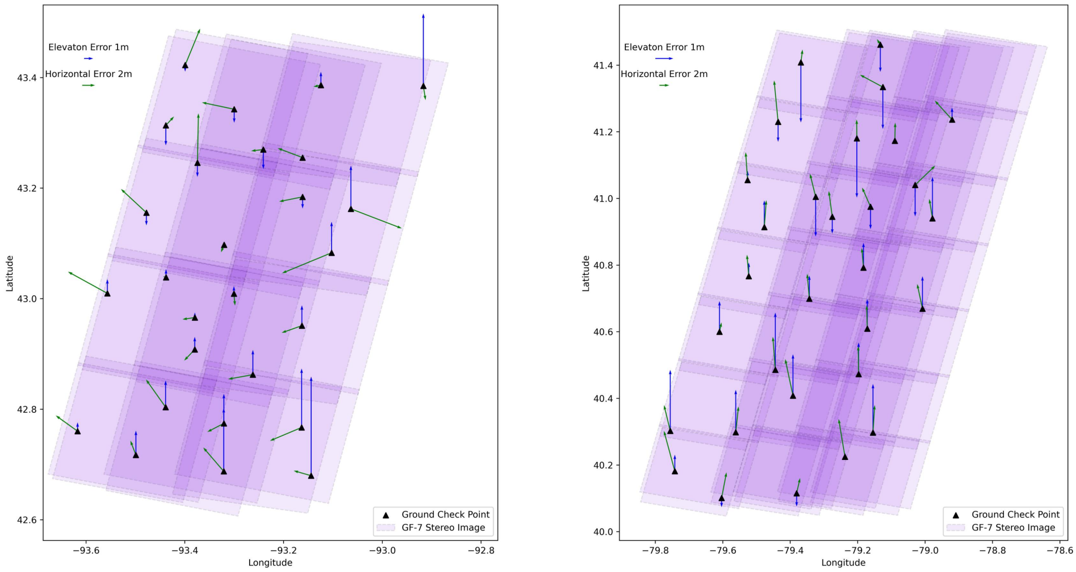

(a)IA survey area (b)PA survey area

Figure 4. Geometric errors of checkpoints for bundle adjustment without laser elevation control points.

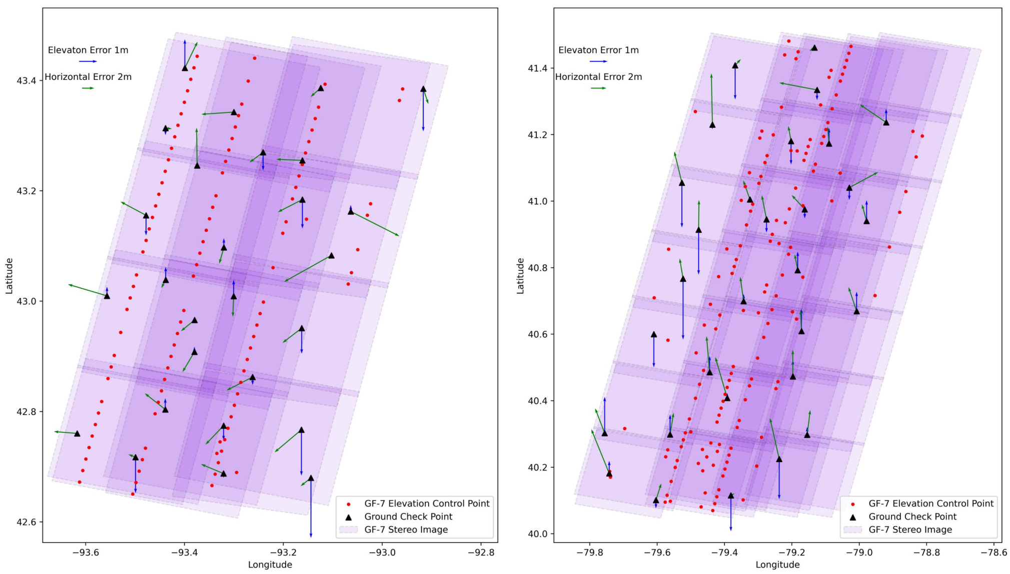

(a)IA survey area (b)PA survey area

Figure 5. Geometric errors of checkpoints for combined bundle adjustment with laser elevation control points from GF-7 satellite.

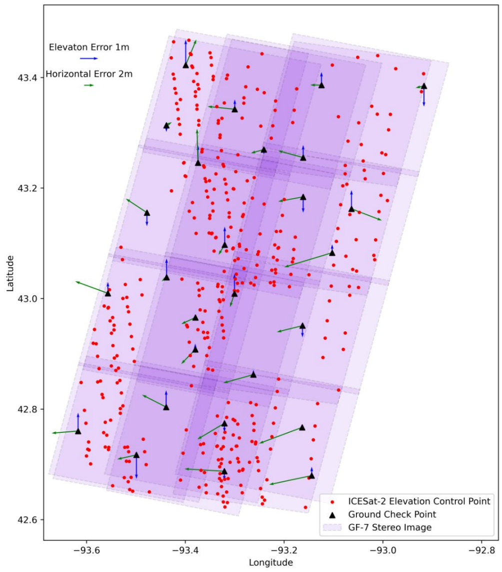

(a)IA survey area

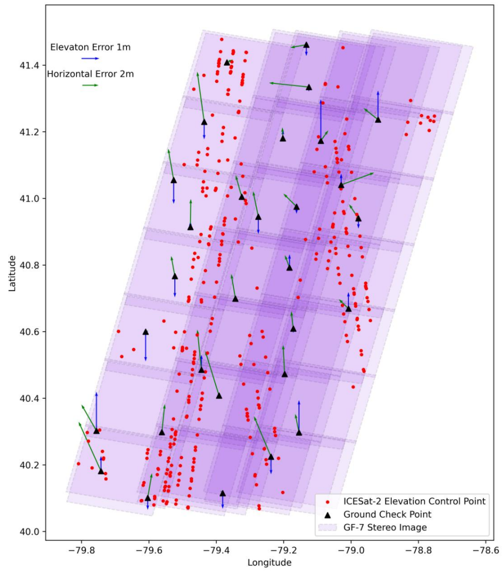

(b)PA survey area

Figure 6. Geometric errors of checkpoints for combined bundle adjustment with laser elevation control points from ICESat-2.

5. Conclusions

In order to compare the effectiveness of optical images stereo mapping in support of laser altimetry data from GF-7 satellite and ICESat-2, this study carried out the extraction of the laser elevation control points and the comparative analysis of the combined bundle adjustment with the GF-7 satellite stereo images. The results reveal that both GF-7 satellite and ICESat-2 laser altimetry data can effectively enhance the accuracy of optical image stereo mapping. Notably, the ICESat-2 satellite laser altimetry data demonstrates superior performance, characterized by its more favorable point density and spatial distribution. Consequently, the combined bundle adjustment of GF-7 satellite stereo images, when integrated with ICESat-2 control points, yields slightly better elevation accuracy across the two survey areas compared to using GF-7 satellite laser altimetry data. Despite the significantly limited capability of the GF-7 satellite in collecting laser elevation control points compared to ICESat-2, it still achieves remarkable performance in elevation control, demonstrating the advantages of stereo mapping by combining optical imagery with laser altimetry data. This limitation will be progressively mitigated as the optimization of future satellite laser altimetry systems, particularly through enhanced laser emission frequencies that promise more sophisticated and dense control point acquisition strategies. Nonetheless, the quantity and distribution of laser elevation control points have significant influences on the results of the combined bundle adjustment. Further research is still needed to comprehensively evaluate the advantages and disadvantages of full-waveform and single-photon counting laser altimetry data in support of stereo mapping with optical imagery.

Acknowledgements

The paper is supported by the National Key Research and Development Program of China (Grant No. 2022YFB3903603) and the National Natural Science Foundation of China (Grant No. 41971425). We would like to express appreciation to the National Aeronautics and Space Administration (NASA) for providing access to the ICESat-2 data.

References

Chen, J.Y., Tang, X.M., Xue, Y.C., Li, G.Y., Zhou, X.Q., Hu, L.R., Zhang, S.T., 2022: Registtion and Combined Adjustment for the Laser Altimetry Data and High-Resolution Optical Stereo Images of the GF-7 Satellite. Remote Sens. 14, 1666.

Dubayah, R., Blair, J.B., Goetz, S., Fatoyinbo, L., Hansen, M., Healey, S., Hofton, M., Hurtt, G., Kellner, J., Luthcke, S., Armston, J., 2020: The Global Ecosystem Dynamics Investigation: High-resolution laser ranging of the Earth's forests and topography. Science of Remote Sensing, p.100002.

Fraser, C.S., Yamakawa, T., 2004: Insights into the affine model for high-resolution satellite sensor orientation. ISPRS Journal of Photogrammetry and Remote Sensing, 58(5-6):275-288.

Huang, G., Ding, Y., Wu, J, 2020: Design and On-orbit Validation of GF-7 Satellite Laser Altimeter. Spacecr. Eng. 3, 68–73.

Li, B.B., Xie, H., Liu, S.J., Tong, X.H., Tang, H., Wang, X., 2021: A Method of Extracting High-Accuracy Elevation Control Points from ICESat-2 Altimetry Data. Photogrammetric Engineering & Remote Sensing. , 87(11): 821 – 830.

Li, G.Y., Tang, X.M, Gao, X.M., Wang, X., Fang, W.F., Chen, J.Y., Mo, F., 2018: Integration of ZY3-02 Satellite Laser Altimetry Data and Stereo Images for High-Accuracy Mapping. Photogrammetric Engineering and Remote Sensing. 84(9):569-578.

Li, G.Y., Tang, X.M., Chen, J.Y., Yao, J.Q., Liu, Z., Gao, X.M., Zuo, Z.Q., Zhou, X.Q., 2021: Processing and preliminary accuracy validation of the GF-7 satellite laser altimetry data. Acta Geodaetica et Cartographica Sinica, 50(10): 1338-1348.

Li, G.Y., Tang, X.M., Zhou, P., Chen, J.Y., Dou, X.H., Liu, Z., Wang, X., 2022: Laser altimetry data processing and combined surveying application of ZY3-03 satellite. Infrared and Laser Engineering, 51(5): 20210356.

Neumann, T.A., Martino, A.J., Markus, T., Bae, S., Bock, M.R., Brenner, A.C., Brunt, K.M., Cavanaugh, J., Fernandes, S.T., Hancock, D.W., 2019: The Ice, Cloud, and Land Elevation Satellite-2 mission: A global geolocated photon product derived from the Advanced Topographic Laser Altimeter System. Remote Sensing of Environment. Volume 233, November, 111325.

Neuenschwander, A., Pitts, K., 2019: The ATL08 Land and Vegetation Product for the ICESat-2 Mission. Remote Sensing of Environment 221: 247 – 259. doi:10.1016/j.rse. 2018.11.005.

Schutz, B.E., Zwally, H.J., Shuman, C.A., Hancock, D., DiMarzio, J.P., 2005: Overview of the ICESat Mission. Geophysical Research Letters. doi: 10.1029/2005GL02400.

Tang, X.M., Xie, J.F., Liu, R. Huang, G.H., Zhao, C.G., Zhen, Y., Tang, H.Z., 2020: Overview of the GF-7 Laser Altimeter System Mission. Earth and Space Science. 7. doi.org/10.1029/2019EA000777.

Tang, X.M, Zhou, P., Guo, L.Y., Pan, H.B., 2023: Integrating Stereo Images and Laser Altimetry Points Derived from the Same Satellite for High-Accuracy Stereo Mapping. Remote Sens. 15, 869.

Wang, M., Wei, Y., Yang, B., Zhou, X., 2021: Extraction and Analysis of Global Elevation Control Points from ICESat-2 /ATLAS Data. Geomatics and Information Science of Wuhan University, 46(2): 184-192.

Zhang, G., Xu, K., Peng, J., Hao, X.Y., Li, D.R. 2019: Integrating Stereo Images and Laser Altimeter Data of the ZY3-02 Satellite for Improved Earth Topographic Modeling. Remote Sensing. 11, 2453.